JACC Vol 7, No 2
February 1986 284–94

Hemodynamic Differentiation of Pathologic and Physiologic Stenosis in Mitral Porcine Bioprostheses

LAWRENCE S. C. CZER, MD, FACC, RICHARD J. GRAY, MD, FACC, TIMOTHY M. BATEMAN, MD, FACC, MICHELE A. DEROBERTIS, RN, KENNETH RESSER, BA, AURELIO CHAUX, MD, FACC, JACK M. MATLOFF, MD, FACC

Los Angeles, California

Porcine bioprostheses are physiologically stenotic valves. Degenerative calcification leading to pathologic stenosis is an increasingly recognized serious late complication of mitral valve replacement with a porcine bioprosthesis. Hemodynamic differentiation of pathologic from physiologic stenosis is important for identification of porcine bioprosthetic valve dysfunction. In 42 patients with a normal Hancock porcine bioprosthesis (standard model, sizes 27 to 33 mm), mean diastolic flow (65 to 461 ml/s), mean gradient (2.0 to 13.4 mm Hg) and effective orifice area (1.1 to 4.4 cm^2) were determined at rest, during epicardial pacing (90, 110 and 130/min) and with isoproterenol infusion. A statistically significant increase in mean gradient occurred with increases in flow and decreases in valve size ($p < 0.05$). Effective orifice area increased significantly as flow rate increased and as valve size increased ($p < 0.05$).

These measurements were compared with those in 16 patients with pathologically confirmed porcine bioprosthetic valve stenosis: 8 patients with reoperation (1.1% per patient-year) 3 to 8.5 years after mitral valve replacement and 8 previously reported abnormal cases. Stenotic failure rate was inversely related to valve size (2.1, 1.4, 0.5 and 0% per patient-year for sizes 27 to 33 mm). Stenotic and normal bioprostheses were not accurately differentiated on the basis of a single value for gradient or effective orifice area. A mathematical model that related flow to the square root of the mean gradient allowed complete separation of stenotic from normal prosthetic valve function, after valve size was accounted for and normal confidence limits were established ($r = 0.74$ to 0.94, sizes 27 to 33, $p < 0.0001$). The effective orifice area-flow relation did not provide accurate differentiation of abnormal from normal function.

Thus, normal mitral bioprostheses have significant transvalvular gradients whose magnitude depends on flow. Risk of stenotic failure is increased in the smaller valves, which have a larger gradient at implantation. Differentiation of pathologic from physiologic stenosis cannot be made on the basis of a single value for gradient or effective orifice area. Accurate hemodynamic differentiation is achieved by relating mean gradient to mean diastolic flow rate and valve size.

(J Am Coll Cardiol 1986;7:284–94)

Glutaraldehyde-preserved porcine bioprostheses are extensively utilized as cardiac valve substitutes because of low thrombogenicity and avoidance of long-term anticoagulation in most patients. The major shortcoming of bioprostheses is their limited durability (1–3), which may be manifested by stenosis, regurgitation or a combination of both (4–13). Prosthetic valve dysfunction due to stenosis is an increasingly recognized late complication after porcine valve replacement, but recognition of stenosis may be difficult because a significant transvalvular gradient has been observed across normal bioprostheses (14–27).

The present study was undertaken to compare the relative hemodynamic performance of normal and stenotic mitral Hancock bioprostheses, and to determine whether reliable hemodynamic differentiation of pathologic from physiologic stenosis could be achieved. In addition, we attempted to determine whether the hemodynamic performance of smaller valve sizes affected long-term stenotic failure rates.

From the Division of Cardiology and Department of Thoracic and Cardiovascular Surgery, Cedars-Sinai Medical Center and Department of Medicine, University of California, Los Angeles School of Medicine, Los Angeles, California. This study was supported in part by Specialized Center of Research on Ischemic Heart Disease Grant HL-17651 from the National Heart, Lung, and Blood Institute, Bethesda, Maryland and by a grant from Mr. and Mrs. Henry Jaffe, Los Angeles, California.

Manuscript received June 25, 1985; revised manuscript received August 29, 1985, accepted September 6, 1985.

Address for reprints: Lawrence S. C. Czer, MD, Cedars-Sinai Medical Center, 8700 Beverly Boulevard, Room 6215, Los Angeles, California 90048.

0735-1097/86/$3 50

Methods

Patients with a normal bioprosthesis. Forty-two consecutive patients undergoing mitral valve replacement with a standard Hancock porcine bioprosthesis (model 342, sizes 27 to 33 mm) were studied within 24 to 48 hours after surgery. Matched length 18 gauge, fluid-filled polyvinyl catheters were placed surgically into the left atrium and left ventricle and were connected to identically calibrated pressure transducers (Honeywell model 4-327-1). Postoperatively, after stabilization and complete rewarming of the patient in the intensive care unit, hemodynamic measurements were performed. These included simultaneous left atrial and left ventricular pressures, cardiac output (by thermodilution), heart rate and diastolic filling period at rest. Measurements were repeated during epicardial atrial pacing (ventricular in three patients) at rates of 90, 110 and 130 beats/min, and after intravenous isoproterenol infusion (concentration 8 μg/ml) at a dose sufficient to increase the heart rate to 120 beats/min (28). The average dose of isoproterenol used was 0.04 μg/kg per min. Pressures were recorded with an Electronics for Medicine VR6 recorder utilizing light-sensitive paper at 100 mm/s. In these 42 normal subjects, a total of 169 studies were performed (mean 4 studies per patient).

Patients with a stenotic bioprosthesis. Of 209 consecutive patients who underwent Hancock porcine mitral valve replacement (model 342, sizes 27 to 33 mm) at Cedars-Sinai Medical Center between 1976 and 1982 and were followed up prospectively for 1 to 100 months (mean 41), 8 (4%) developed worsening symptoms and a new diastolic murmur suggestive of bioprosthetic valve stenosis. Each of these patients underwent cardiac catheterization.

Simultaneous left ventricular and pulmonary capillary wedge pressures (corrected for phase delay), cardiac output (by thermodilution), heart rate and diastolic filling period were measured at rest and with transvenous atrial pacing at 110 beats/min or with isoproterenol infusion (8 μg/ml at a dose sufficient to increase heart rate to 120 beats/min) if these interventions were deemed clinically safe. In these eight patients, 15 studies were performed (mean 2 studies per patient).

An additional group of eight patients with mitral Hancock bioprosthetic valve stenosis and corresponding cardiac catheterization data were obtained by a review of the literature (29–34). In this group eight studies were available. Thus, in a total of 16 patients with a stenotic prosthesis (8 of our own and 8 from published reports), 23 hemodynamic studies were available. All 16 patients underwent reopera-

Table 1. Hemodynamic Data at Baseline and After Interventions in 42 Patients With a Normal Hancock Mitral Bioprosthesis (sizes 27 to 33 mm)

Hemodynamic Variable	Baseline (n = 51)	Intervention: Pacing (90/min) (n = 34)	Intervention: Pacing (110/min) (n = 35)	Intervention: Pacing (130/min) (n = 29)	Intervention: Isoproterenol (n = 20)
Mean diastolic flow (ml/s)					
Mean ± SD	138 ± 49	160 ± 43	201 ± 45*	230 ± 52*	289 ± 85*
Range	65 to 251	88 to 271	121 to 303	137 to 375	157 to 461
Mean gradient (mm Hg)					
Mean ± SD	3.6 ± 1.8	3 7 ± 1.4	5.6 ± 2.1*	7.1 ± 2.3*	7 8 ± 3.0*
Range	2.0 to 8.4	2.0 to 7 2	2.0 to 10 5	4.0 to 13.0	2 0 to 13.4
Effective orifice area (cm^2)					
Mean ± SD	1.95 ± 0.50	2.25 ± 0.55*	2.32 ± 0.58*	2.32 ± 0 54*	2.82 ± 0.76*
Range	1 10 to 3 46	1.24 to 3.72	1 64 to 3.89	1.63 to 4.00	1.82 to 4 40
Stroke volume (ml)					
Mean ± SD	50 ± 12	46 ± 11	41 ± 9*	34 ± 6*	64 ± 16*†
Diastolic filling period (seconds/beat)					
Mean ± SD	0.39 ± 0 11	0.29 ± 0.04*	0 21 ± 0 03*	0.15 ± 0.03*	0.23 ± 0 06*†
Heart rate (min^{-1})					
Mean ± SD	80 ± 16	90 ± 2*	110 ± 4*	129 ± 3*	118 ± 20*
Rhythm					
Sinus	32	0	0	0	13
Atrial fibrillation	11	0	0	0	5
Atrial-paced	8	31	33	27	2
Ventricular paced	0	3	2	2	0
Left atrial pressure (mm Hg)					
Mean ± SD	13.2 ± 4.1	15.5 ± 4.6	16.2 ± 4.7*	16.7 ± 4.2*	15.3 ± 4.5

*$p < 0.05$, compared with baseline value; †$p < 0.05$, isoproterenol for pacing at 130/min.

tion, explantation and pathologic examination of the bioprosthetic valve, with confirmation of pathologic stenosis in each patient.

Etiologic classification of stenosis. The cause of the bioprosthetic valve stenosis was determined from gross anatomic, microscopic and radiographic examination of the excised prosthesis (4–11). *Calcification* was considered to be the cause of stenosis if multiple firm, nodular masses ($\geq$ 2 mm) adherent to the leaflet base, body or edge of all three leaflets and resulting in restricted leaflet excursion were identified. Histologic and ex vivo radiographic evidence of calcification was judged confirmatory.

Fibrous tissue overgrowth was identified as the cause of stenosis if the inflow orifice of the anulus was covered by a layer of connective tissue that extended at least 2 mm onto the base of all three leaflets, reducing the size of the inflow orifice and restricting leaflet mobility. Frequently, the outflow surface of the leaflet was covered by fibrous tissue as well. Microscopic findings of a collagenous sheath that covered relatively normal-appearing leaflet tissue was judged confirmatory.

Prosthetic valve thrombosis was considered to be the cause of stenosis if a thrombus adherent to the inflow surface of a leaflet produced orifice narrowing, or if the thrombus was identified on the outflow surface of the leaflet and resulted in restriction of leaflet mobility. *Inward stent bending* was considered the cause of stenosis if the polypropylene stents were bent inward, producing orifice narrowing (29).

Calculations. Mean diastolic pressure gradient (G) was determined from the area, measured by planimetry, between the simultaneous diastolic left ventricular and left atrial (or phase-corrected pulmonary capillary wedge) pressures, divided by the diastolic filling period per beat (defined by the crossover of left atrial and left ventricular pressures). In the presence of atrial fibrillation, the mean gradient was averaged over 10 beats.

Mean diastolic flow (ml/s) was calculated from the cardiac output (CO), heart rate (HR) and diastolic filling period per beat (DFP) according to the formula: mean diastolic flow = CO/(HR $\times$ DFP).

Effective orifice area (EOA) was calculated from the Gorlin relation according to the formula: EOA = mean diastolic flow/(38 $\times$ $\sqrt{G}$).

Statistical methods. Values of continuous variables are expressed as mean $\pm$ SD. Comparisons between continuous variables for two groups were made with the unpaired two-tailed *t* test. Comparisons among continuous variables for three or more groups were made with Friedman's nonparametric analysis of variance, and pairwise comparisons utilized the Wilcoxon signed-rank test with alpha levels adjusted by applying the Bonferroni correction. Comparisons across flow ranges and valve sizes were made using Kruskal-Wallis one-way analysis of variance; differences were isolated using Fisher's least significant difference method applied to ranks. Discrete variables were compared by means of chi-square analysis or Fisher's exact test. For all univariate analyses, the alpha level was set at 0.05. Linear regression analysis was performed by the methods of least squares. All statistical calculations were performed by BMDP statistical software (35–37).

Results

Normal Bioprostheses

Diastolic flow, diastolic gradient and effective orifice area (Table 1). At the baseline level of mean diastolic flow (138 $\pm$ 49 ml/s; range 65 to 251), the mean diastolic pressure gradient was 3.6 $\pm$ 1.8 mm Hg (range 2.0 to 8.4) and the effective orifice area was 1.95 $\pm$ 0.50 cm^2 (range 1.10 to 3.46). To extend the range of flows over which observations were made, measurements were repeated with epicardial pacing at incrementally increasing rates and after infusion of isoproterenol. At paced rates of 110 and 130 beats/min, there was a statistically significant increase in mean diastolic flow, mean gradient and effective orifice area compared with values at rest ($p < 0.05$). Mean diastolic flow increased despite a decrease in stroke volume and this increase was associated with marked shortening of the diastolic filling period ($p < 0.05$). Pacing at 90 beats/min produced an intermediate response.

Figure 1. Influence of valve size and flow rate on mean diastolic pressure gradient. There was a statistically significant decrement in gradient from the smallest (27 mm) to the largest (33 mm) valve size at each flow interval (50 to 150, 151 to 250 and 251 to 350 ml/s). For each valve size there was a significant increase in gradient with increasing flow. **Asterisk** indicates a statistically significant difference when compared with the gradient at a flow rate of 50 to 150 ml/s.

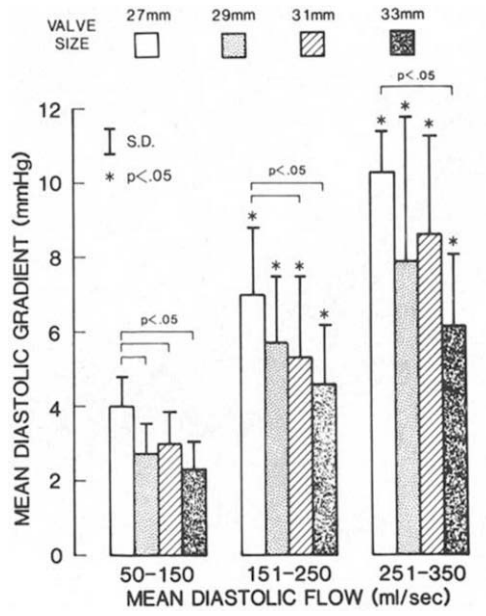

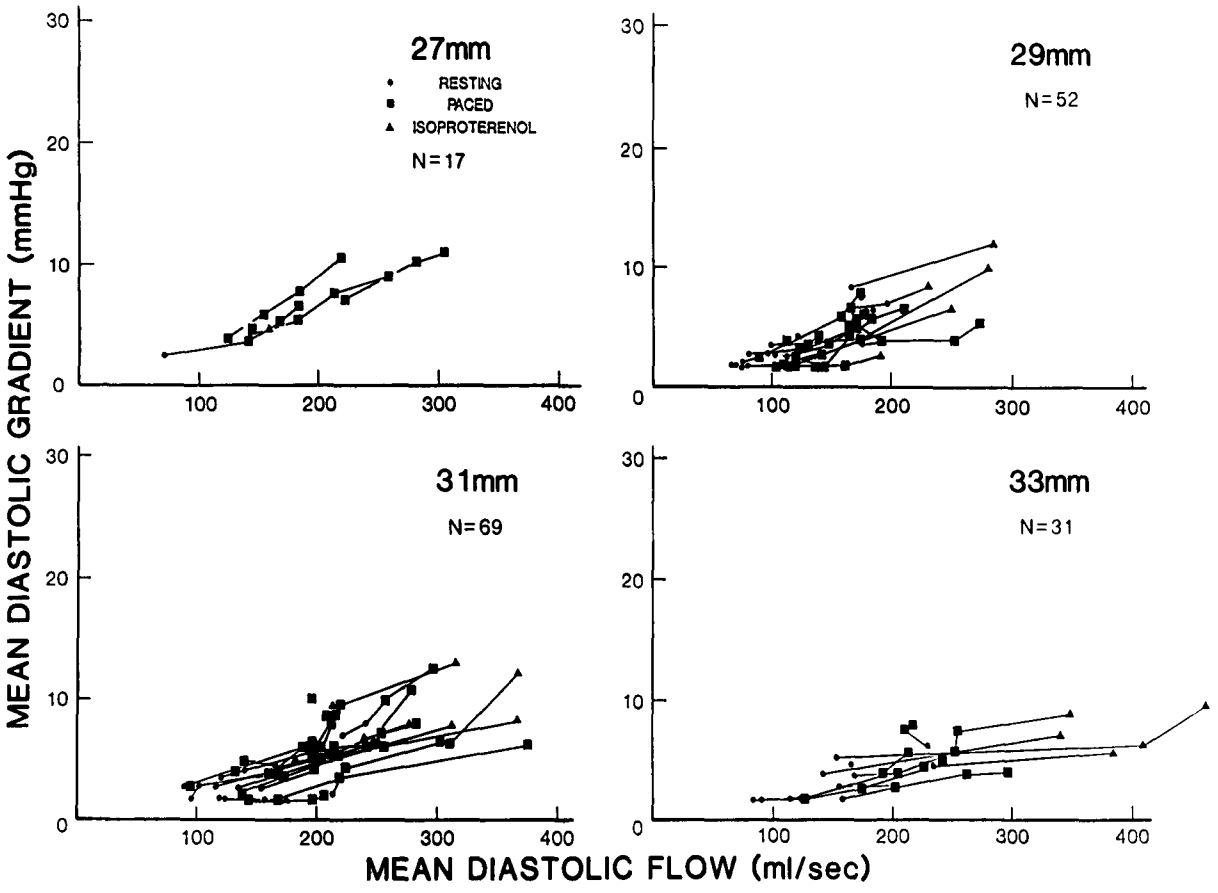

Figure 2. Gradient-flow relation in normal Hancock bioprostheses, stratified by valve size. **Solid line** connects mean pressure gradients measured across an individual valve at different flow rates produced by varying conditions (**symbols**). In general, mean gradient increased as flow increased. This increase was least pronounced in the largest valve size (33 mm).

Isoproterenol (average dose 0.04 μg/kg per min) produced the largest mean diastolic flow (289 ± 85 ml/s), gradient (7.8 ± 3.0 mm Hg) and effective orifice area (2.82 ± 0.76 cm^2). These values were somewhat larger than, but statistically not different from, those obtained with pacing at 130 beats/min. With isoproterenol, the increase in mean diastolic flow was associated with an increase in stroke volume and a lesser shortening of the diastolic filling period compared with the value during pacing at 130 beats/min ($p < 0.05$) (Table 1).

Gradient-flow relation. Because interventions that increased flow were associated with concomitant increases in gradient (Table 1), we investigated more closely this correlation and its relation to valve size. A statistically significant ($p < 0.05$) difference in mean gradient was observed between the smallest (27 mm) and largest (33 mm) valve size at each of three defined flow intervals (Fig. 1). For each valve size, there was a statistically significant increase

Figure 3. Influence of valve size and flow rate on effective orifice area. There was a statistically significant increase in effective orifice area from the smallest (27 mm) to the largest (33 mm) valve size at each flow interval (50 to 150, 151 to 250 and 251 to 350 ml/s). For each valve size there was a significant increase in effective orifice area with increasing flow. **Asterisk** indicates a statistically significant difference when compared with effective orifice area at a flow rate of 50 to 150 ml/s.

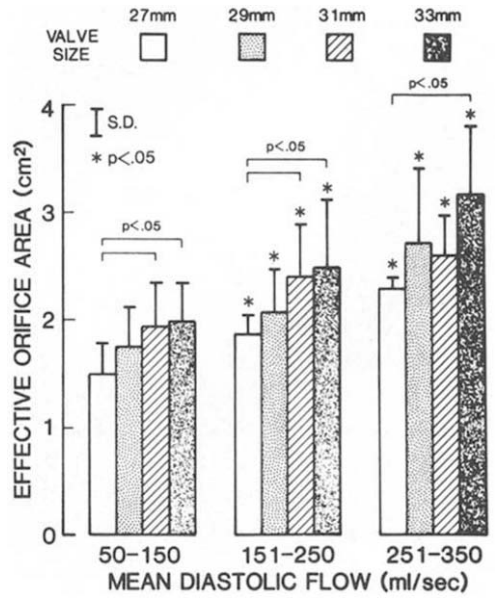

JACC Vol 7, No 2
February 1986 284–94

in mean gradient at medium (150 to 250 ml/s) and high (250 to 350 ml/s) flow rates, compared with the gradient at a low flow rate (50 to 150 ml/s). Thus, the mean gradient across a normal bioprosthesis was substantially influenced by both flow rate and valve size.

This effect was confirmed on an individual basis (Fig. 2). Interventions that increased flow generally increased mean gradient, but to a much lesser extent in larger valves. The largest valve (33 mm) had the largest maximal flows (400 to 500 ml/s) with the smallest gradients. Additionally, the largest flows were observed in the largest valves.

Effective orifice area-flow relation. Effective orifice area, calculated according to the Gorlin relation, differed significantly in the smallest and largest valves (Fig. 3). For each valve size there was a statistically significant ($p < 0.05$) increase in the effective orifice area at medium (150 to 250 ml/s) and high (250 to 350 ml/s) flows, compared with that at a lower flow rate (50 to 150 ml/s). On an individual basis interventions that increased flow led in most cases to an increase in effective orifice area (Fig. 4). A linear regression model confirmed a statistically significant correlation between effective orifice area and valve flow ($r = 0.55$ to 0.89, $p < 0.001$ for each valve size) (Fig. 5).

Stenotic Bioprostheses

Stenotic failure rate (Table 2). In our entire series of patients with mitral Hancock valves (n = 209), the linearized stenotic failure rate was 1.1% per patient-year of follow-up (8 events). The stenotic failure rate was highest in the smaller valves (2.1 and 1.4% per patient-year for sizes 27 and 29 mm, respectively) and lowest in the larger valves (0.5 and 0% per patient-year for sizes 31 and 33 mm, respectively). Stenotic failure also related to longer implant duration: four failures occurred in the cohort whose valve had been in place for 7 to 8 years, three in the cohort operated on 5 to 6 years previously, one in the 3 to 4 year cohort and none in the cohort operated on within the preceding 2 years.

Etiology of stenosis. The predominant cause of bioprosthetic valve stenosis was extensive leaflet calcification,

Figure 4. Effective orifice area-flow relation in normal Hancock bioprostheses stratified by valve size. **Solid line** connects effective orifice area calculated for an individual valve at different flow rates under varying conditions (**symbols**). In general, effective orifice area increased as flow increased. The most marked increase was observed in the largest valve size (33 mm).

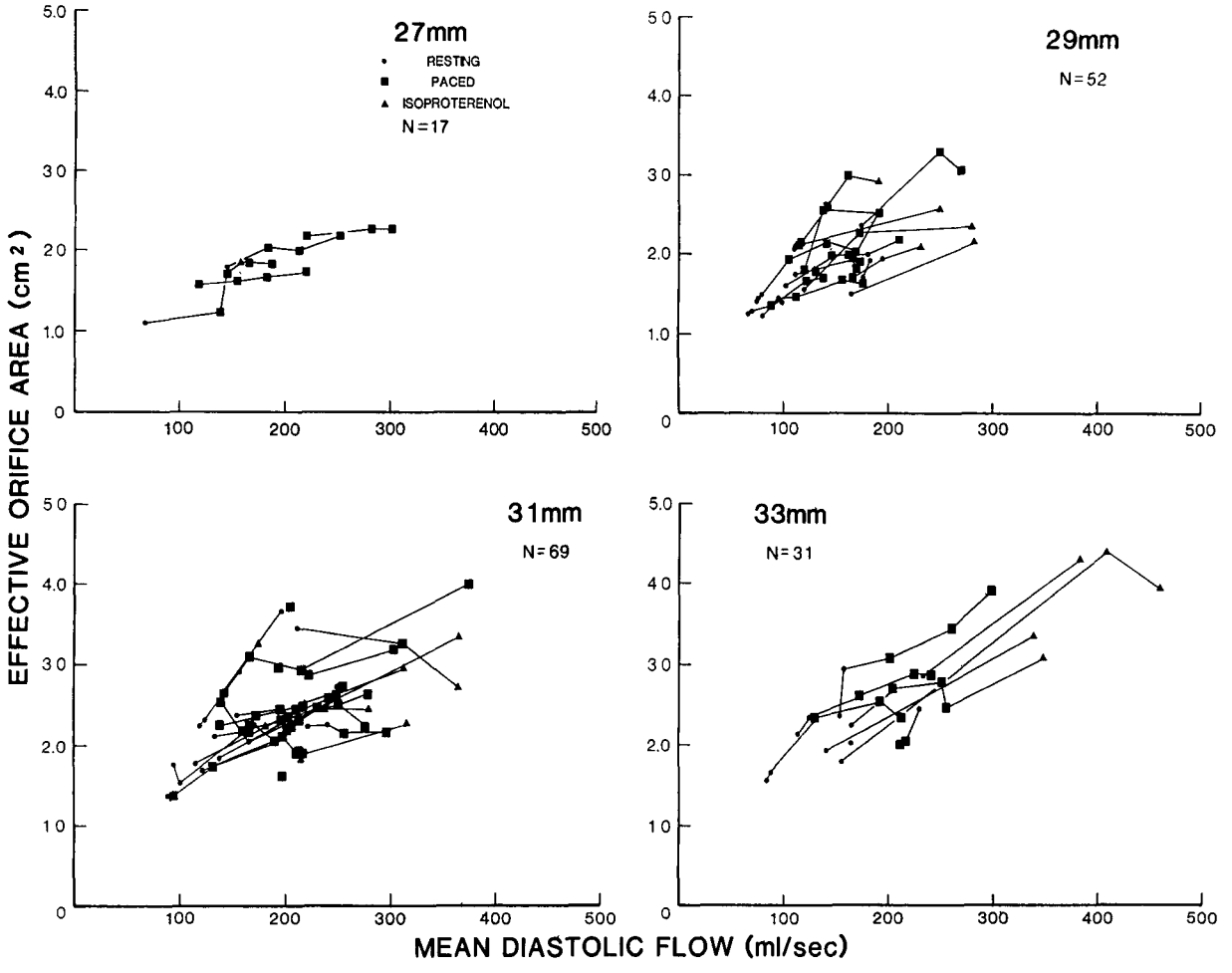

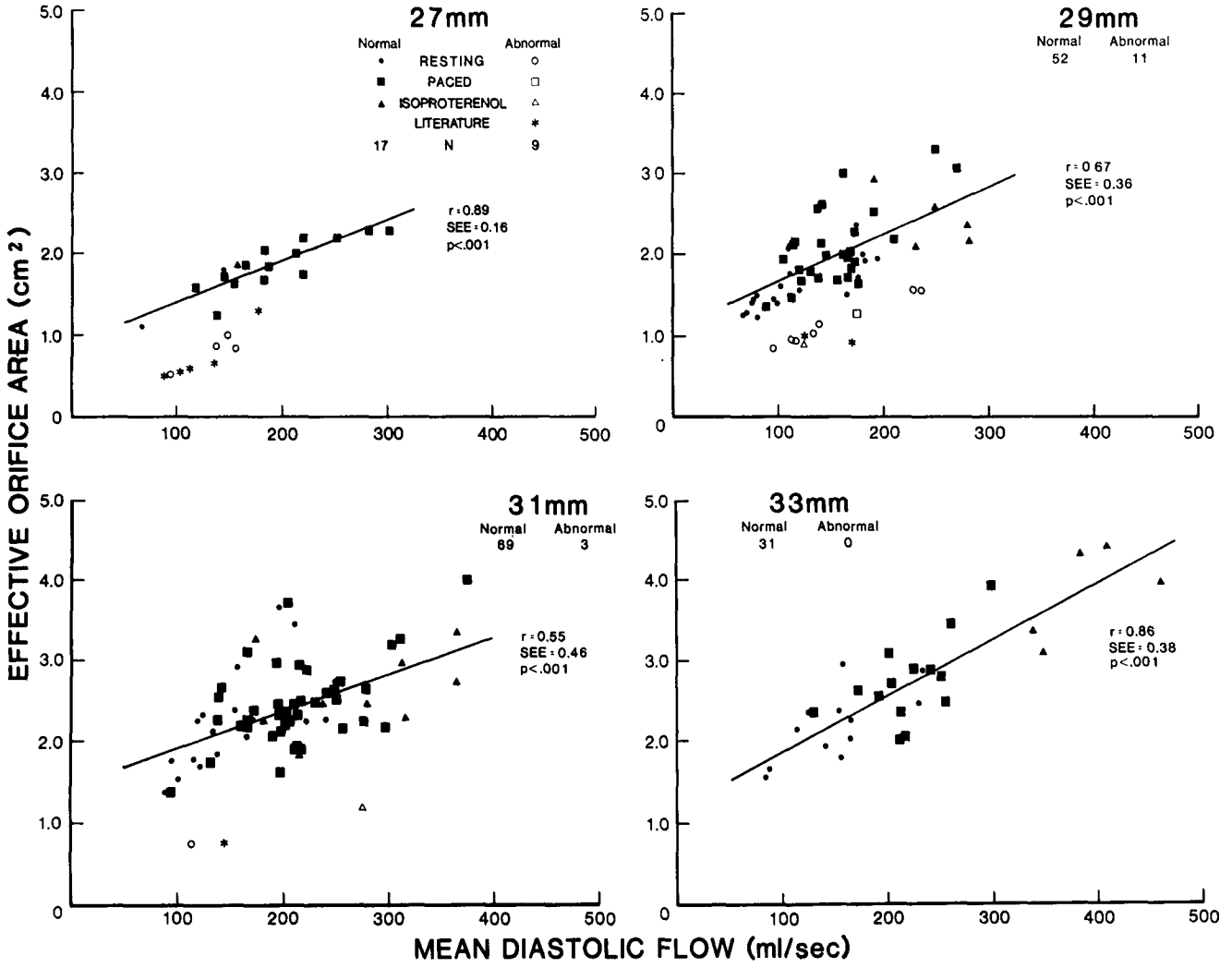

Figure 5. Comparison of effective orifice area-flow relation in normal (**solid symbols**) and stenotic (**open symbols** and **asterisks**) Hancock bioprostheses by valve size. Effective orifice area was less suitable than gradient for differentiation of abnormal from normal function (see text).

Table 2. Stenotic Failure Rates in 209 Patients After Mitral Valve Replacement With a Hancock Porcine Bioprosthesis (1976 to 1982)

Valve Size (mm)	No. of Patients	Follow-Up (mo)* Mean (range)	Stenotic Failures: Events	Stenotic Failures: Rate per 100 Patient-Years
27	40	43 (1 to 78)	3	2 1
29	78	43 (1 to 95)	4	1 4
31	67	39 (1 to 101)	1	0 5
33	24	36 (1 to 86)	0	0
27 to 33	209	41 (1 to 101)	8	1.1

*Follow-up 96% complete (eight lost).

which occurred in four (50%) of eight patients. Fibrous tissue overgrowth into the inflow orifice and onto the base of the leaflets was observed in three (38%) of eight whereas prosthetic thrombosis or inward stent bending occurred in one (12%) of eight.

Hemodynamic findings (Table 3). Cardiac catheterization before reoperation demonstrated a mean diastolic gradient of 16 ± 8 mm Hg (range 9 to 38) at a mean diastolic flow of 152 ± 55 ml/s (range 94 to 228), with a calculated effective orifice area of 1.0 ± 0.3 cm^2 (range 0.5 to 1.5).

Previously reported cases of stenotic valve failure (Table 3). The valve size distribution, interval to explantation, pathologic findings and hemodynamics of the eight reported abnormal valves (29–34) were similar to those of our own eight stenotic bioprostheses. The only statistically significant difference was age. Our patients with an abnormal valve were older than those reported on previously but were significantly younger than the remaining patients at our institution who did not develop bioprosthetic valve stenosis ($p < 0.05$). Because of the similarity in pathologic and hemodynamic findings, both groups of stenotic bioprostheses were pooled for the purpose of comparison with the normal valves.

Table 3. Clinical Characteristics of Patients With a Stenotic Hancock Mitral Bioprosthesis From Present Series (n = 8) and From Literature Review (n = 8)

	Present Series (n = 8)	Previously Reported Cases† (n = 8)
Age at implantation (yr)*		
Mean ± SD	51 ± 13	23 ± 17
Range	25 to 66	6 to 50
Valve size (mm)		
27	3	5
29	4	2
31	1	1
33	0	0
Interval to explantation (mo)		
Mean ± SD	72 ± 19	51 ± 33
Range	39 to 96	4 to 106
Hemodynamics before explantation		
Mean diastolic gradient (mm Hg)		
Mean ± SD	16 ± 8	22 ± 7
Range	9 to 38	11 to 30
No. of studies performed	15	8
Effective orifice area (cm^2)		
Mean ± SD	1.0 ± 0.3	0.8 ± 0.3
Range	0.5 to 1.5	0.5 to 1.3
No. of studies performed	15	8
Mean diastolic flow (ml/s)		
Mean ± SD	152 ± 55	132 ± 30
Range	94 to 228	91 to 178
No. of studies performed	15	8
Pathologic mode of failure		
Leaflet calcification	4	4
Fibrous tissue overgrowth	3	3
Inward stent bending	0	1
Thrombosis	1	0

*$p < 0.05$, present series versus previously reported cases; †references 29 to 34.

Differentiation of pathologic from physiologic stenosis

Abnormal valves had a significantly larger mean gradient, smaller effective orifice area and lower flow than normal valves ($p < 0.05$) (Table 4). However, no single value of gradient or effective orifice area completely differentiated stenotic from normal valves because of overlap in the hemodynamics of these two groups. For example, choosing 13 mm Hg as the upper limit of normal for the gradient falsely classified 9 of 23 abnormal measurements as normal (39% false negative rate). If the upper limit of normal was decreased to 12 or 11 mm Hg, the false negative rate was reduced, but the false positive rate (identification of normal valves as stenotic) was increased. We believed that the diagnostic accuracy of these measurements might be improved if flow and valve size were taken into account.

A linear regression model identified in normal valves a statistically significant ($p < 0.0001$) correlation between flow and square root of the gradient; the mean regression line was an exponential function when plotted as gradient versus flow (Fig. 6). The predicted gradient-flow relation was different for each valve size; larger valve sizes demonstrated smaller gradients at equivalent flow rates. The mean regression equations for gradient (G) as a function of flow in valves of various size were given by the following formulas: $\sqrt{G} = 0.0079 \times \text{flow} + 1.08$ (27 mm; $r = 0.94$, $p < 0.0001$); $\sqrt{G} = 0.0075 \times \text{flow} + 0.89$ (29 mm; $r = 0.78$, $p < 0.0001$); $\sqrt{G} = 0.0066 \times \text{flow} + 0.93$ (31 mm; $r = 0.74$, $p < 0.0001$); $\sqrt{G} = 0.0040 \times \text{flow} + 1.23$ (33 mm; $r = 0.76$, $p < 0.0001$).

Ninety-nine percent confidence limits for gradient as a function of flow were constructed from the regression model. These confidence limits (dotted lines in Fig. 6) were chosen to minimize the misclassification of normal and abnormal valves, because it was perceived that reoperation in patients with a normal valve was more harmful than delaying operation in patients with a slightly stenotic valve. All measurements in stenotic valves fell outside the 99% confidence limits of the gradient-flow relation for each valve size, and all values in normal valves were within these limits (Fig. 6). Therefore, complete differentiation of stenotic from normal measurements was achieved, and the misclassification rate was reduced to zero.

A linear regression model identified a significant correlation between effective orifice area and flow (Fig. 5). However, there was a greater degree of data scatter than occurred for the gradient-flow relation and, as a result, the confidence limits were relatively wide and overlapped with some of the abnormal values. Accordingly, the effective orifice area-flow relation was not suitable for complete differentiation of abnormal from normal function.

Discussion

Normal bioprosthetic function. Hancock porcine bioprostheses are physiologically stenotic valves. In vitro (14–17) and in vivo (18–27) studies have demonstrated that Hancock bioprostheses produce larger gradients, smaller effective orifice areas and larger transvalvular energy losses than mechanical tilting disc (Björk-Shiley, Lillehei-Kaster) and bileaflet (St. Jude) valves of comparable anular dimensions.

Table 4. Gradient, Effective Orifice Area and Flow in Normal and Stenotic Mitral Hancock Bioprostheses

	Normal (n = 169)	Stenotic (n = 23)	p Value
Mean gradient (mm Hg)			
Mean ± SD	5.2 ± 2.6	18.3 ± 7.6	< 0.05
Range	2.0 to 13.4	9.0 to 38.0	
Effective orifice area (cm^2)			
Mean ± SD	2.3 ± 0.6	0.9 ± 0.3	< 0.05
Range	1.1 to 4.4	0.50 to 1.5	
Mean diastolic flow (ml/s)			
Mean ± SD	189 ± 72	145 ± 48	< 0.05
Range	65 to 461	91 to 278	

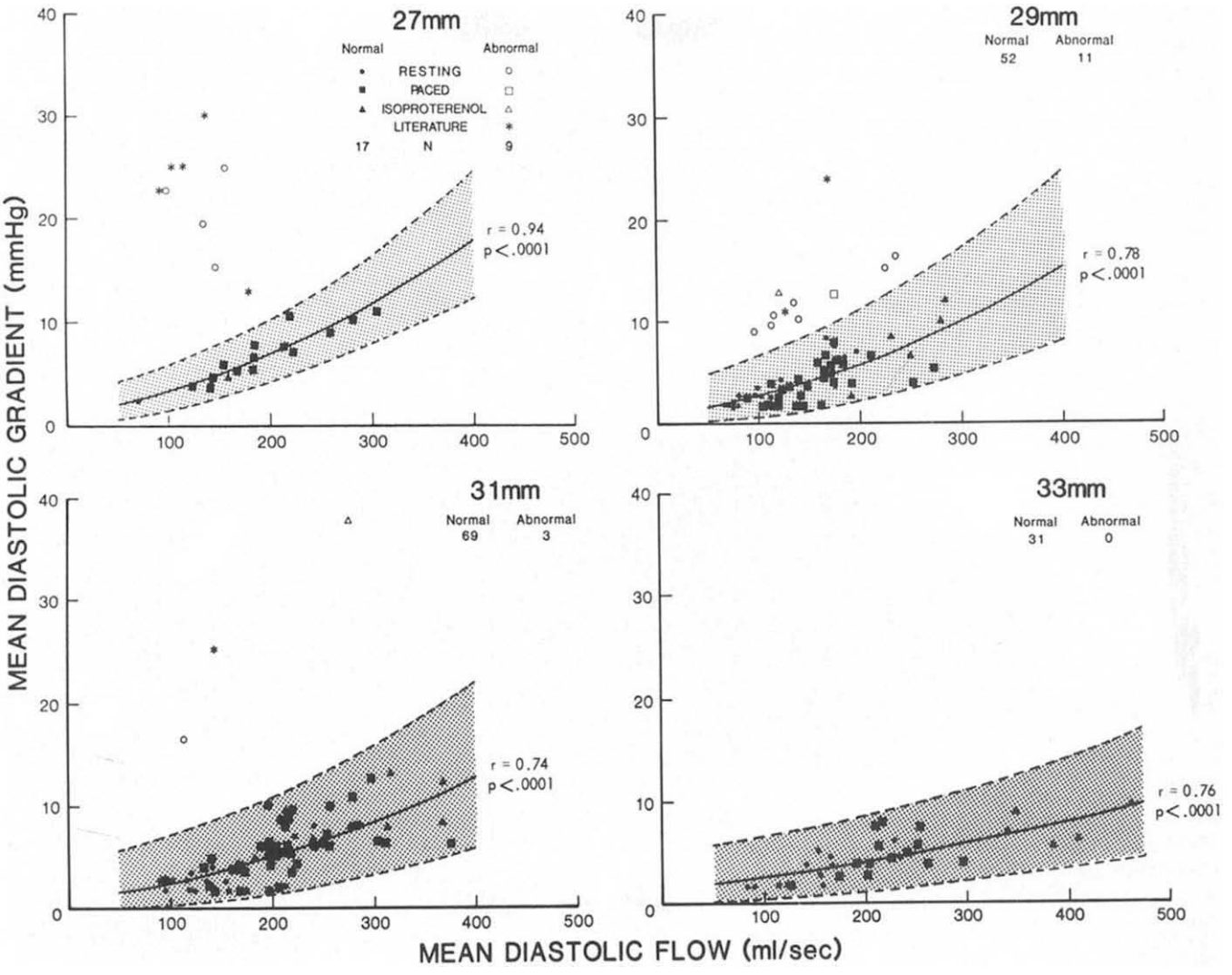

Figure 6. Comparison of gradient-flow relation in normal and stenotic Hancock bioprostheses, stratified by valve size. The **dashed lines** outline the 99% confidence limits of the normal gradient-flow relation, between which (**shaded area**) are contained all 169 measurements from 42 normal valves (**solid symbols**). Note that all 23 measurements in 16 stenotic valves (**open symbols** and **asterisks**) are **above** and to the **left** of the **shaded area**.

The reason is that the supporting structures of the Hancock valve (sewing ring, struts and muscle shelf) occupy a larger proportion of the available anular area, resulting in a smaller ratio of the internal to external orifice area (14–17,38). It has been anticipated that the larger gradients may be physiologically important, especially in the smaller sizes of the Hancock valve (1–3,23).

In normal mitral Hancock valves, the present study demonstrated mean pressure gradients ranging from 2.0 to 8.4 mm Hg at mean diastolic flow rates of 65 to 251 ml/s (Table 1). Ubago et al. (19) reported a mean gradient of 18.3 mm Hg across a normal mitral Hancock valve (size 27 mm) and other studies (18–27) have documented a wide range of normal gradients. Because flow rates as high as 419 ml/s occur under baseline conditions (19), we performed incremental epicardial pacing (22) and isoproterenol infusion (24) to extend the range of flows over which observations were made, and to determine whether an increase in flow produced an increase in mean gradient in vivo. Our study demonstrated that interventions that increased flow led to an increase in gradient; isoproterenol infusion generally produced the largest increment in mean diastolic flow and mean gradient (Table 1). On an individual basis, incremental increases in flow were accompanied by incremental increases in mean gradient, regardless of the type of intervention (Fig. 2).

A mathematical model that correlated mean diastolic flow with the square root of the gradient fit the data well ($r = 0.74$ to 0.94, $p < 0.0001$) after significant differences according to valve size were accounted for (Fig. 1 and 6). This allowed determination and construction of the confidence limits of the normal gradient-flow relation in vivo for each valve size. Importantly, all normal values obtained in this study fell within these confidence limits (Fig. 6).

Effective orifice area increased with higher flow rates (Fig. 4 and 5), after differences due to valve size were

JACC Vol 7, No 2
February 1986 284–94

accounted for (Fig. 3). Previous in vitro and in vivo studies (14,17,19) have corroborated these findings. Wright (15) demonstrated that the mitral Hancock valve does not open fully until peak pulsatile flow exceeds 165 to 238 ml/s (for sizes 27 to 33 mm). At lower peak pulsatile flow rates, the valve remains incompletely open throughout diastole. At higher peak pulsatile flow rates, the valve opens fully only during that part of diastole in which the flow rates exceed these threshold levels. Thus, leaflet pliability determines the extent and duration of maximal leaflet opening.

Phasic variations in orifice size are apparent throughout diastole when bioprostheses are photographed by high-speed cinematography (14,15). Porcine bioprostheses therefore behave as dynamic rather than static orifices. Fisher et al. (39) emphasized the need to adjust for variations in size during phasic mitral flow to obtain the mean orifice area.

Viscous effects (15,17) contribute another source of variation of effective orifice area with flow. These effects are most prominent at low flow rates, where they add to the pressure gradient and reduce effective orifice area. At very high flows, their contribution is negligible. Thus, when viscous effects are accounted for, effective orifice area gradually increases with flow, eventually reaching a plateau as the orifice area approaches a certain limit (17).

The discharge coefficient utilized in the Gorlin relation is very close to 1 for nearly all bioprostheses (15,17), but may vary with flow and gradient, especially at the extremes of flow. Therefore, the use of a fixed constant in the calculation of mean effective orifice area may lead to significant errors in estimation of the true orifice area. Indeed, a greater degree of data scattering and smaller correlation coefficients were observed in the effective orifice area-flow relation (Fig. 5) compared with the gradient-flow relation. In addition, because effective orifice area is a calculated (not measured) entity, errors are compounded. Because of all these considerations, the effective orifice area-flow relation was not suitable for establishment of normal limits.

Bioprosthetic stenosis. In pathologic studies of of porcine bioprostheses removed at surgery or necropsy (4–11), calcification was the most common degenerative process leading to valve dysfunction. The two principal sites of calcification were the connective tissue and the cusps (particularly along the collagen fibrils in the spongiosa), and small thrombi on the surface of the cusps (6). These calcific deposits caused cuspal stiffening and ultimately stenosis, or collagen disruption leading to possible tears and regurgitation. Bioprosthetic stenosis, although most commonly caused by calcification, may also result from thrombosis, fibrous tissue overgrowth, large vegetations and strut creep (9,10,12,13,29–34).

In long-term follow-up of large patient series (40–43), bioprosthetic valve degeneration has occurred at a rate of 2 to 3% per patient-year, with an actuarial freedom from degeneration of 71 to 79% at 10 years. Higher rates of tissue failure have been observed in younger age groups, especially children (40,43–48), and in valves that have been implanted for more than 5 years (12,42). Bioprostheses demonstrate more severe pathologic changes and a higher incidence of failure in the mitral than in the aortic position; this may be due to a larger pressure difference and a greater tensile stress on the cusps when closed, and more frequent flexion when open (twice per cycle) compared with the aortic position (12,49–51).

In the present study of 209 recipients of a Hancock mitral valve followed up for up to 8.5 years, the stenotic failure rate was 1.1% per patient-year. This stenotic failure rate was related inversely to valve size, being four times more likely in the 27 mm than in the 31 mm valve (Table 2). Thus, the larger gradients and less efficient hemodynamic performance of the smaller valves translated into a higher risk of stenotic failure. It may be logically concluded that a small mitral anulus is a relative contraindication to the use of a bioprosthesis.

Each of the eight stenotic bioprostheses described in this report underwent explantation and pathologic examination. The predominant mode of failure was leaflet calcification (Table 3), which has been the experience at other centers (4–13,40–49). In comparison with the eight patients in published reports of pathologically confirmed bioprosthetic stenosis accompanied by preoperative catheterization studies (29–34), the eight patients in our study were older, but otherwise had a similar valve size distribution, interval to explantation, hemodynamic profile before explantation and pathologic mode of failure. Thus, our experience with bioprosthetic stenosis was quite similar to that previously reported.

Hemodynamic differentiation of pathologic from physiologic stenosis. Given the wide range of gradients that may be found with normally functioning Hancock bioprostheses, and the small gradients that may occur in stenotic valves at low flow rates, hemodynamic differentiation of pathologic from physiologic stenosis on the basis of a single value of gradient or effective orifice area may be difficult. The cost of an incorrect diagnosis is likely to be quite high: the patient with an incorrect diagnosis of prosthetic stenosis may undergo an unnecessary operation with attendant morbidity and mortality, while the patient incorrectly judged to have a normal valve may have unexplained severe symptoms for many years. Furthermore, as the time interval from implantation increases, a greater number of patients may be expected to come to medical attention because of suspected bioprosthetic stenosis (42).

Importantly, the normal gradient-flow relation, when stratified by valve size (Fig. 6), completely differentiated stenotic from normally functioning valves. These limits, established early postoperatively during the first 2 years of our experience with the Hancock valve, were prospectively validated by comparison with data on stenotic bioprostheses

later obtained from our own patient group (minimal interval to explantation, 3 years) and from previously reported cases (29–34), all of which had hemodynamic values outside the normal gradient-flow limits.

The effective orifice area-flow relation provided less reliable discrimination (Fig. 5) because of a greater degree of data scattering in normal valves. This variability in the effective orifice area-flow relation might be decreased by taking into account the gradient- or flow-dependence of the Gorlin constant (52), but this approach has not been validated in porcine bioprostheses under conditions of phasic mitral flow. The equation for adjustment of the Gorlin constant is likely to be different in stenotic and normal prostheses (52), a distinction that is usually not known a priori. Errors in gradient or flow determination will be compounded by such an adjustment in the calculation of effective orifice area. For all of these reasons, we have found that the gradient-flow relation is a better discriminator between normal and stenotic function than is the effective orifice area-flow relation.

Lipson et al. (53) reported a significant increase in mean gradient and decrease in effective orifice area as determined by cardiac catheterization in 18 patients with a Hancock mitral valve in place for more than 5 years. Only one of these patients underwent reoperation, explantation and pathologic examination of the prosthesis. Whether most of these patients simply developed progressive cuspal stiffening due to increasing leaflet thickness (54,55) or whether they developed true pathologic stenosis due to extensive leaflet calcification, thrombosis or strut creep cannot be determined from their study. In the single patient who underwent reoperation, pathologic stenosis due to strut creep was identified; the preoperative hemodynamic measurements (mean gradient 12 mm Hg; flow 158 ml/s; size 29 mm) were clearly outside the normal range established in our study. Although cuspal stiffening may theoretically be problematic for the definition of normal hemodynamics, the choice of 99% confidence limits (as in our study) probably results in the classification of all such patients as "normal." Such a classification may be justified, given the risks of reoperation in these patients with minimally abnormal valves.

Role of alternative diagnostic approaches. Bioprosthetic valve stenosis cannot be reliably assessed by history, physical examination or current noninvasive techniques (1,53). Spectral phonocardiographic changes in the peak frequency of the first heart sound may be a manifestation of leaflet stiffening or stenosis (56), but the accuracy and reproducibility of the technique are unknown and its validity has not been established by pathologic examination of large numbers of excised bioprostheses. Similarly, two-dimensional echocardiographic assessment of bioprosthetic mitral valve stenosis is not reliable; significant stenosis may be missed, and stenosis may be falsely identified when not present (57).

Doppler ultrasound techniques provide a noninvasive estimation of blood flow velocity and pressure gradients across bioprosthetic valves (58–60), and this method appears promising in the evaluation of bioprosthetic valve stenosis. However, such gradients measured across normal and stenotic valves may demonstrate sizable overlap (60). The results of the present study suggest that such measurements will not be very useful in distinguishing abnormal from normal function unless measurement of transvalvular flow is available. Unfortunately, significant technical problems remain with Doppler-derived cardiac output determinations (39). Pressure half-time may provide an improved Doppler assessment of prosthetic stenosis, but experience with this technique in mitral valve bioprostheses has been limited and requires further evaluation (59).

We gratefully acknowledge the secretarial assistance of Helen Schamroth and Kathie Farrington. Graphic illustrations were provided by Lance LaForteza

References

1. Rahimtoola SH. Valvular heart disease: a perspective. J Am Coll Cardiol 1983;1:199–215.
2. Carpentier A, Dubost C, Lane E, et al. Continuing improvements in valvular bioprostheses. J Thorac Cardiovasc Surg 1982;83:27–42.
3. Angell WW, Angell JD. Porcine valves. Prog Cardiovasc Dis 1980;23:141–66.
4. Fishbein MC, Gissen SA, Collins JJ Jr, Barsamian EM, Cohn LH. Pathologic findings after cardiac valve replacement with glutaraldehyde-fixed porcine valves. Am J Cardiol 1977;40:331–7.
5. Ferrans VJ, Spray TL, Billingham ME, Roberts WC. Structural changes in glutaraldehyde-treated porcine heterografts used as substitute cardiac valves. Am J Cardiol 1978;41:1159–84.
6. Ferrans VJ, Boyce SW, Billingham ME, Jones M, Ishihara T, Roberts WC. Calcific deposits in porcine bioprostheses: structure and pathogenesis. Am J Cardiol 1980;46:721–34.
7. Ishihara T, Ferrans VJ, Boyce SW, Jones M, Roberts WC. Structure and classification of cuspal tears and perforations in porcine bioprosthetic cardiac valves implanted in patients. Am J Cardiol 1981;48:665–78.
8. Cipriano PR, Billingham ME, Oyer PE, Kutsche LM, Stinson EB. Calcification of porcine prosthetic heart valves: a radiographic and light microscopic study. Circulation 1982;66:1100–4.
9. Camilleri JP, Pomin B, Carpentier A. Structural changes of glutaraldehyde-treated porcine bioprosthetic valves. Arch Pathol Lab Med 1982;106:490–6.
10. Valente M, Bortolotti U, Arbustini E, Talenti E, Thiene G, Galluci V. Glutaraldehyde-preserved porcine bioprosthesis: factors affecting performance as determined by pathologic studies. Chest 1983;83:607–11.
11. Schoen FJ, Levy RJ. Bioprosthetic heart valve failure: pathology and pathogenesis. In: Waller B, ed. Cardiology Clinics. Cardiac Morphology. Vol 2. Philadelphia: WB Saunders, 1984:717–8.
12. Schoen FJ, Collins JJ Jr, Cohn LH. Long-term failure rate and morphologic correlations in porcine bioprosthetic heart valves. Am J Cardiol 1983;51:957–64.
13. Platt MR, Mills LJ, Estrera AS, Hillis LD, Buja LM, Willerson JT. Marked thrombosis and calcification of porcine heterograft valves. Circulation 1980;62:862–9.
14. Walker DK, Scotten LN, Modi VJ, Brownlee RT. In vitro assessment of mitral valve prostheses. J Thorac Cardiovasc Surg 1980;79:680–8.
15. Wright JTM. Hydrodynamic evaluation of tissue valves. In: Ionescu M, ed. Tissue Heart Valves. London: Butterworth, 1979.29–87.
16. Gabbay S, McQueen DM, Yellin EL, Frater RWM. In vitro hydro-

dynamic comparison of mitral valve prostheses at high flow rates. J Thorac Cardiovasc Surg 1978;76.771–87

17 Gabbay S, McQueen DM, Yellin EL, Frater RWM. In vitro hydrodynamic comparison of mitral valve bioprostheses Circulation 1979;60(suppl I):I-62–70

18. Levine FH, Carter JE, Buckley MJ, Daggett WM, Akins CW, Austen WG. Hemodynamic evaluation of Hancock and Carpentier-Edwards bioprostheses. Circulation 1981;64(suppl II):II-192–5.

19. Ubago JL, Figueroa A, Colman T, Ochoteco A, Duran CG Hemodynamic factors that affect calculated orifice areas in the mitral Hancock xenograft valve. Circulation 1980;61.388–94.

20. Holen J, Hoie J, Semb B Obstructive characteristics of Björk-Shiley, Hancock and Lillehie-Kaster prosthetic mitral valves in the immediate postoperative period. Acta Med Scand 1978;204:5–10.

21. Lurie AJ, Miller RR, Maxwell KS, et al. Hemodynamic assessment of the glutaraldehyde-preserved porcine heterograft in the aortic and mitral positions. Circulation 1977;56(suppl II):II-104–10.

22. Johnson AD, Daily PO, Peterson KL, et al. Functional evaluation of the porcine heterograft in the mitral position. Circulation 1975, 51,52(suppl I):I-40–8.

23. Johnson A, Thompson S, Vieweg WVR, Daily P, Oury J, Peterson K. Evaluation of the in vivo function of the Hancock porcine xenograft in the aortic position. J Thorac Cardiovasc Surg 1978;75:599–605.

24. Borkon AM, McIntosh CI, Jones M, Lipson LC, Kent KM, Morrow AG Hemodynamic function of the Hancock standard orifice aortic valve bioprosthesis. J Thorac Cardiovasc Surg 1981,82:601–7.

25. Hannah H III, Reis RL. Current status of porcine heterograft prostheses. Circulation 1976;54(suppl III):III-27–31.

26. Cevese PG, Gallucci V, Morea M, Volta SD, Fasoli G, Casarotto D. Heart valve replacement with the Hancock bioprosthesis. Circulation 1977;56(suppl II):II-111–6.

27. Jones EL, Craver JM, Morris DC, et al. Hemodynamic and clinical evaluation of the Hancock xenograft bioprosthesis for aortic valve replacement (with emphasis on management of the small aortic root). J Thorac Cardiovasc Surg 1978;75:300–8

28. Gray RJ, Chaux A, Matloff JM, et al. Bileaflet, tilting disc and porcine aortic valve substitutes: in vivo hydrodynamic characteristics. J Am Coll Cardiol 1984;3:321–7.

29. Borkon AM, McIntosh CL, Jones M, Roberts WC, Morrow AG. Inward stent-post bending of a porcine bioprosthesis in the mitral position. J Thorac Cardiovasc Surg 1982;83:105–7.

30. Curcio CA, Commerford PJ, Rose AG, Stevens JE, Barnard MS. Calcification of glutaraldehyde-preserved porcine xenografts in young patients. J Thorac Cardiovasc Surg 1981;81:621–5. (Patient 4)

31. Lamberti JJ, Wainer BH, Fisher KA, Karunaratne HB, Al-Sadir J. Calcific stenosis of the porcine heterograft. Ann Thorac Surg 1979;28:28–32.

32. Bortolotti U, Galluci V, Casarotto D, Thiene G. Fibrous tissue overgrowth on Hancock mitral xenografts: a cause of late prosthetic stenosis. Thorac Cardiovasc Surg 1979;27:316–8. (Cases 1 and 2)

33. Sanders SP, Levy RJ, Freed MD, Norwood WI, Castaneda AR. Use of Hancock porcine xenografts in children and adolescents. Am J Cardiol 1980;46:429–38. (Cases 18 and 21)

34. Horowitz MS, Goodman DJ, Fogarty TJ, Harrison D. Mitral valve replacement with the glutaraldehyde-preserved porcine heterograft. J Thorac Cardiovasc Surg 1974;67:885–95. (Patient D.M.K.)

35. Dixon WJ, ed. BMDP Statistical Software. Los Angeles: University of California Press, 1981:1–725

36. Draper N, Smith H Applied Regression Analysis New York: John Wiley & Sons, 1981:1–265.

37. Conover W. Practical Nonparametric Statistics. New York: John Wiley & Sons, 1980:144–299.

38. Gabbay S, Yellin EL, Frishman WH, Frater WRM. In vitro hydrodynamic comparison of St. Jude, Björk-Shiley and Hall-Kaster valves. Trans Am Soc Artif Intern Organs 1980;26:231–5.

39 Fisher DC, Sahn DJ, Friedman MJ, et al. The mitral valve orifice method for noninvasive two-dimensional echo Doppler determinations of cardiac output. Circulation 1983,67.872–7.

40 Magilligan DJ, Lewis JW Jr, Tilley B, Peterson E. The porcine bioprosthetic valve. J Thorac Cardiovasc Surg 1985;89.499–507.

41. Gallucci V, Bortolotti U, Milano A, Valfre C, Mazzucco A, Thiene G. Isolated mitral valve replacement with the Hancock bioprosthesis: a 13-year appraisal. Ann Thorac Surg 1984;38:571–8.

42. Gallo I, Ruiz B, Nistal F, Duran C. Degeneration in porcine bioprosthetic cardiac valves: incidence of primary tissue failures among 938 bioprostheses at risk. Am J Cardiol 1984;53:1061–5.

43. Craver JM, Jones EL, McKeown P, Bone DK, Hatcher CR Jr, Kandrach M. Porcine cardiac xenograft valves: analysis of survival, valve failure, and explanation. Ann Thorac Surg 1982;34:16–21.

44 Williams DB, Danielson GK, McGoon DC, Puga FJ, Mair DD, Edwards WD. Porcine heterograft valve replacement in children. J Thorac Cardiovasc Surg 1982;84:446–50

45. Miller DC, Stinson EB, Oyer PE, et al The durability of porcine xenograft valves and conduits in children. Circulation 1982;66(suppl I).I-172–85.

46. Wada J, Yokoyama M, Hashimoto A, et al. Long-term follow-up of artificial valves in patients under 15 years old. Ann Thorac Surg 1980;29:519–21

47. Kutsche LM, Oyer P, Shumway N, Baum D. An important complication of Hancock mitral valve replacement in children. Circulation 1979;60(suppl I).I-98–103.

48. Geha AS, Laks H, Stansel HC Jr, et al. Late failure of porcine valve heterografts in children. J Thorac Cardiovasc Surg 1979;78:351–64.

49. Warnes CA, Scott ML, Silver GM, Smith CW, Ferrans VJ, Roberts WC. Comparison of late degenerative changes in porcine bioprostheses in the mitral and aortic valve position in the same patient. Am J Cardiol 1983;51.965–8.

50. Thubrikar M, Piepgrass WC, Deck JD, Nolan SP. Stress of natural versus prosthetic aortic valve leaflets in vivo. Ann Thorac Surg 1980;30:230–9.

51. Sabbah HN, Hamid MS, Stein PD. Estimation of mechanical stresses on closed cusps of porcine bioprosthetic valves: effects of stiffening, focal calcium and focal thinning. Am J Cardiol 1985;55:1091–6.

52. Cannon SR, Richards KL, Crawford M. Hydraulic estimation of stenotic orifice area: a correction of the Gorlin formula. Circulation 1985;71:1170–8.

53. Lipson LC, Kent KM, Rosing DR, et al. Long-term hemodynamic assessment of the porcine heterograft in the mitral position. Circulation 1981;64:397–402

54. Alam M, Goldstein S, Lakier JB. Echocardiographic changes in the thickness of porcine valves with time. Chest 1981;79:663–8.

55. Forman MB, Phelan BK, Robertson RM, Virmani R. Correlation of two-dimensional echocardiography and pathologic findings in porcine valve dysfunction. J Am Coll Cardiol 1985;5:224–30.

56. Stein PD, Sabbah HN, Lakier JB, Magilligan DJ Jr, Goldstein S. Frequency of the first heart sound in the assessment of stiffening of mitral bioprosthetic valves. Circulation 1981;63:200–3.

57. Grenadier E, Sahn DJ, Roche AHG, et al. Detection of deterioration or infection of homograft and porcine xenograft bioprosthetic valves in mitral and aortic positions by two-dimensional echocardiographic examination J Am Coll Cardiol 1983;2:452–9.

58. Ramirez ML, Wong M. Reproducibility of stand-alone continuous-wave Doppler recordings of aortic flow velocity across bioprosthetic valves. Am J Cardiol 1985;55.1197–9.

59. Ryan T, Armstrong WF, Dillon JC, Feigenbaum H. Doppler evaluation of patients with porcine mitral valves (abstr). J Am Coll Cardiol 1985;5:526

60. Hatle L, Angelsen B. Doppler Ultrasound in Cardiology: Physical Principles and Clinical Applications. Philadelphia: Lea & Febiger, 1985:189–96.